Chapter 1
General Introduction

General Introduction

1.1. Small is Different: A Brief Introduction to Nanoparticles

Nanoscience and nanotechnology are current inventive branches of sciences and technology that are developing at a very fast pace.[1,2] Particles with at least one of the dimensions in the range of 1−100 nm, so called nanomaterials, are larger than individual atoms and smaller than the bulk solids.[3] Therefore, particles in the nanometer length scale, exhibit interesting optical, electronic, catalytic, and magnetic properties with varying size, shape/morphology and dispersity that are, surprisingly, different from the corresponding individual atoms and the complement bulk solids.[4-6] With decreasing the size of the particles to nanoscale dimension, the 'surface-to-volume' ratio of the nanoparticles sharply increases and exhibits quantum size effect.[7] Generally, metals have properties which are termed as "metallic properties" that includes conduction of heat and electricity, do not have any band gap between valence band and conduction band, are good conductor of heat and electricity and do not exhibit any characteristic colour in their bulk state. The significant changes in optical and electronic properties with shrinking the sizes of the solids to the nano-dimension are governed by the variation of sizes and shape of the nanostructures. The interesting exhibition of characteristic optical and electronic characteristics of the coinage metals in their nanoscale dimension has been of considerable interest in recent times. Moreover, the physicochemical behaviour of the nanosurfaces has significant contribution in the structural features of the surfaces and the mechanism of the surface reactions that has attracted considerable interest in the technological developments of the new generation of functional devices.

Noble metal nanoparticles, i. e., gold, silver and copper display characteristic absorption band in the UV-vis-NIR region due to the absorption of electromagnetic radiation (photon) by the surface electrons below the de-Broglie wavelength region and start oscillating that have been coined as surface plasmon resonance (SPR). The sharpness or broadness of the optical absorption band of the nanoparticles varies with the size and shape/morphology of the particles and has enable for applications, involving, light-metal interactions in a new field known as plasmonics.[1, 8-12] In plasmonics, metal

nanostructures can serve as antennas through a strong interaction between incident light and free electrons in the nanostructures to convert light with effective manipulation into localized electric fields or as waveguides to route light to desired locations with nanometer precision.[10,13] Nanoparticles of noble metal demonstrate widely interesting morphology-dependent optical, electronic and chemical properties which are, further, accelerated on functionalization by different organic fluorophores attached chemically/physically onto the surface of nanoparticles to exploit the role in photophysical processes. Moreover, gold and silver are able to survive in the nanoscale dimension under atmospheric conditions as they are noble enough and the versatile chemistry available for surface functionalization makes the materials suitable for possible ligand binding.[14]

1.1.1. Optical and Electronic Properties of Nanoparticles

Nanoparticles are comprised of a large number of atoms or molecules bonded together and may be distributed in gaseous, liquid or in solid substances. The interesting properties of nanoscale materials are depending upon the number of surface atoms and the surface area which are specified as intrinsic size effects and extrinsic size effects. Intrinsic size effects concern specific changes in volume and surface material properties. Experimentally, they deal with electronic and structural properties, namely, ionization potentials, binding energies, chemical reactivity, crystallographic structure, melting temperatures, and optical properties of metal clusters that depend upon the particle size and geometry. [14-15] As the particle size increases, the energy levels continue to split and finally merge into the quasi-continuous band structure in the bulk solid. The spacing of energy level in metal is shown in Figure 1.1. The splitting patterns in energy level arising due to the discretion (quantization) of electron energy levels, are known as quantum size effects. For small sizes of the particles, the optical properties become size dependent, whereas for larger ones, the electrodynamic

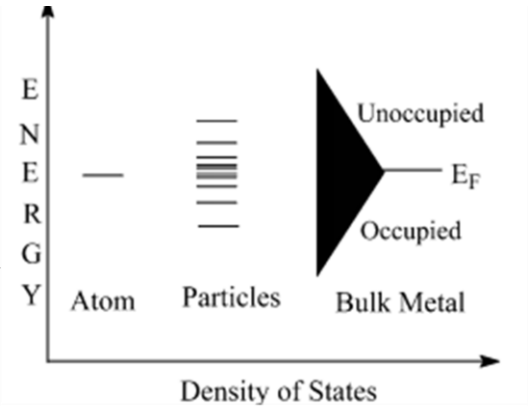

Figure 1.1. Energy levels in metal particles.

theory can be applied using bulk optical constants, and this is known as extrinsic size effect.

The variation of exhibited color of colloidal gold with particle size of the metal nanoparticles was explained by Gustav Mie in 1908 applying the general theory of light extinction to small particles using the electrodynamics.[16] The theory describes the extinction (absorption and scattering) of spherical particles of arbitrary sizes. The excellent color of colloidal gold and its variation with size of the particles can be explained, theoretically, by considering the interaction of light with metal cluster bearing spherical geometry by solving Maxwell's equations for the incident light. For a spherical shaped particle with arbitrary sizes, Mie theory gives the extinction cross-section, $\sigma_{ext.}$ For a particle of radius r, it could be expressed in the form of following equation,

$$\sigma_{ext} = 9\frac{\omega}{c}\epsilon_m^{3/2}V_0\frac{\epsilon_2(\omega)}{[\epsilon_1(\omega)+2\epsilon_m]^2+\epsilon_2(\omega)^2} \quad (1.1)$$

where, $V_0 = \frac{4}{3}\pi r^3$, the volume of the particle, ω, the angular frequency of the exciting light, $\epsilon_1(\omega)$ and $\epsilon_2(\omega)$ are the real and imaginary components of the dielectric function of the metal, i. e., $\epsilon(\omega) = \epsilon_1(\omega) + i\epsilon_2(\omega)$ and ϵ_m, the real dielectric of the medium. The extinction, σ_{ext}, contributed from absorption and scattering of the particles, i. e., $\sigma_{ext} = \sigma_{abs} + \sigma_{scat}$ of a metal nanosphere. Mie theory is strictly applicable only to spherical particles. For spheroidal shaped particles, smaller then the wavelength of light, Gans theory provides an analytical expression and the extinction spectra could be calculated. For other anisotropic shaped nanostructures, numerical approximations, like, discrete dipole approximation, finite-difference time-domain methods have been used for the calculations of extinction spectra.

1.2. Fluorescent Probes

The functionalization and surface engineering of nanostructures with fluoroprobe molecules would be a model system in 3-D arrangements around the nanoparticles by forming the organic–inorganic nanoscale assemblies for understanding the effect of metal-probe interactions. Modification of the surface of metal nanoparticles with fluorophores containing different functional groups, such as, thiols, amines, or silanes to attach onto the nanosurface is essential for the development of biological traces, optoelectronic devices, efficient light-energy conversion systems, data storage and

sensors.[17] Organic fluorescent dye molecules have numerous applications in different fields of sciences, like, surface chemistry, microscopy, chemical analysis, and medicines.[5] Since fluorescence spectroscopy is a very sensitive technique, organic fluoroprobes have, often, been attached onto the surfaces of plasmonic metal to study the surface behavior of nanostructures using fluorescence spectroscopy that facilitated the measurement of molecular level interactions on/at the surfaces. Semiconductor quantum dots have also been attached onto the surface of the metal to study the rate of emission properties, the electron transfer process and band gap modulation.[18] The decreases in the fluorescence intensity onto the surface of the metallic particles are due to the decrease in radiative decay rate of the fluorophores.[19] The enhancement of fluorescence intensity due to the intensification of the incoming electric field because of the formation of the 'hot spot' in the nanostructures.[20] The study of surface plasmon coupling of radiative molecules to metallic surfaces has started at the beginning of the 20th century with the theoretical work by Zenneck and Sommerfeld, among others.[21, 22] It was realized that the emission of fluorophore near metal surfaces would lead to directional and polarized emission because the propagating electromagnetic fields of surface plasmons at interfaces propagate with a preferred direction and polarization. Subsequently, the intrinsic isotropic fluorescence emission of randomly oriented fluorophores above surfaces would directionally emit by coupling to the surface plasmons of the metal nanosurfaces.[23]

1.3. Physical Parameters affecting Nanoparticle-Fluoroprobe Interaction

Coinage metal particles, at the nanoscale dimension, exhibit excellent extinction coefficient having size and morphology−dependent tuneability of the absorption spectra over the UV-vis-NIR region with various characteristic colors and noble enough to survive as a nanoparticke under atmospheric conditions. Moreover, the surface modification by different functional groups has paved an avenue towards the formation of metal-probe hybrid assemliess and therefore, to investigate the mechanistic details of the various deactivation pathways. A number of plausible physical parameters have been believed to be involved in the formation of metal-fluoroprobe hybrid assemblies. The surface-to-volume ratio of the nanoparticles, residual force of nanostructures, temperature, roughness of the metal surface, chain length and functional groups of surface capping, solvent dielectrics, polarisability of the functional group of fluoroprobe

molecules, types (physio/chemi) of adsorbate-surface interaction, pH, concentration and presence of foreign ions in the colloidal solution are thought to be the major effect in nanoparticle-fluorophore assembly formation.[14, 24, 25]

1.4. Theoretical Background

A large number of theoretical studies (this list is far from complete) have been performed over the last few decades in understanding the behavior of fluoroprobe molecules in which the molecular dipole is damped by the presence of a nearby metal surface. These theories of surface spectroscopy account for three elements into consideration: the local electromagnetic field acting on each molecule, the molecular response to this field, and the emission by the polarized molecule. All steps of a surface chemical reaction—sticking, reaction and desorption— involve energy exchange between the adsorbate and substrate states.

Theory of Energy Transfer

Energy transfer is a powerful technique which has been widely used in applications of fluorescence, DNA analysis, medical diagnostics, sensing, structure determination, gene therapy, drug delivery and optical imaging[26-29] energy transfer occurs as a radiationless process from a donor fluorophore to an acceptor that could be another flurophore of lower energy, a metal nanoparticle, a metal film, or a dark quencher. The nature and the efficiency of energy transfer depend on the photophysical properties of the donor fluorophores, acceptors and the neighboring environments. There are several models/ theories of energy transfer which have been developed based on different assumptions.[28] The general representation of the rate of energy transfer, k_T, between the donor and acceptor is dependent on their optical properties, the distance of separation,[28] R_0, and can be expressed as,

$$k_T(r) = \frac{1}{\tau_D}\left(\frac{R_0}{r}\right)^n \qquad (1.2)$$

where, τ_D is the excited state lifetime of the donor dye in the absence of acceptor, R_0 is the distance at which efficiency of energy transfer is 50%, also called the 'critical distance' and n is a fitting parameter. Both R_0 and n are highly dependent on the nature of the donor and acceptor with n being a function of the dimensions of the donor and acceptor, where, R_0 directly relates to the photophysical constants for the donor and

acceptor. Several theories have been developed to explain the nature and conditions of energy transfer for the donor-acceptor pair systems, such as, FRET,[30] Gersten-Nitzan theory,[31] CPS-Kuhn model[32] and NSET.[33] These energy transfer mechanisms have been elucidated from the description of relevant theories, their assumptions and limiting conditions as stated in the following paragraphs. Some of the important theories/models have been briefly described below.

1.4.1. Förster Resonance Energy Transfer

The elegant theory of transfer of energy, known as Förster Resonance Energy Transfer (FRET) was developed in 1948 by Professor Theodor Förster to explain the rate of fluorescence resonance energy transfer between a donor and an acceptor.[30] This theory assumes the dipole-dipole interaction between a fluorescent donor and an acceptor molecule of point dipoles and predicts a $1/R^6$ dependence of rate of energy transfer in center-to-center separation distance, *R*. Moreover, a pre-averaging over the orientations of the two dipoles is considered and has contribution in rate of energy transfer. The extent of FRET is readily predictable from the spectral overlap between the donor emission and absorption of the acceptors. FRET occurs between a donor fluorophore (D) in the excited state and ground state acceptor (A) molecule and not due to absorption of photon emitted from donor fluorophore but is the result of dipole–dipole interactions between the donor and acceptor. The energy transfer rate depends upon the extent of spectral overlap between donor emission and acceptor absorption, the quantum yield of the donor, extinction of the acceptor, the relative dipole orientation of the donor and acceptor, and the distance between the donor and acceptor molecules.

The rate of Förster resonance energy transfer (non-radiative) for a donor and acceptor separated by a distance *r* is given by,

$$k_T(r) = \frac{Q_D \kappa^2}{\tau_D r^6}\left(\frac{9000(ln10)}{128\pi^5 N_A \eta^4}\right) J(\lambda) = \frac{1}{\tau_D}\left(\frac{R_0}{r}\right)^6 \qquad (1.3)$$

where,Q_D is the quantum yield of the donor in the absence of acceptor, η the refractive index of the medium, N_A Avogadro's number, r the distance between the donor and acceptor, τ_D the excited-state radiative lifetime of the donor in absence of acceptor, and R_0 the Förster separation and $J(\lambda)$ the overlap integral between the emission spectrum of donor fluorophore and absorption spectrum of acceptor molecule. The term, κ^2 is

describing the relative orientation in space of the transition dipoles of the donor and acceptor with respect to each other, such that, $\kappa = cos\theta_T - 3cos\theta_D cos\theta_A$ where, θ_T is the angle between the emission transition dipole of the donor and the absorption transition dipole of the acceptor, θ_D and θ_A are the angles between these dipoles and the vector joining the donor and the acceptor. The value of κ can vary from 0 to 4 depending on the relative orientation of the donor and the acceptor and usually assumed to be equal to 2/3, which is appropriate for dynamic random averaging of the donor and acceptor. The overlap integral, $J(\lambda)$ expresses the extent of spectral overlap between the emission of donor fluorophore and absorption spectrum of the acceptor molecules and could be written as[28]

$$J(\lambda) = \int_0^\infty F_D\,(\lambda)\varepsilon_A(\lambda)\lambda^4 d\lambda = \frac{\int_0^\infty F_D(\lambda)\varepsilon_A(\lambda)\lambda^4 d\lambda}{\int_0^\infty F_D(\lambda)d\lambda} \tag{1.4}$$

where, $F_D(\lambda)$ is the corrected fluorescence intensity of the donor in the wavelength range $\lambda$to $\lambda + \Delta\lambda$ with the total intensity (area under the curve) normalized to unity, $\varepsilon_A(\lambda)$ the extinction co-efficient of the acceptor at λ, which is typically in units of M^{-1} cm^{-1} and $F_D(\lambda)$ is dimensionless. If $\varepsilon_A(\lambda)$ is expressed in units of M^{-1} cm^{-1} and λ is in nanometers, then $J(\lambda)$ is in units of M^{-1} cm^{-1} nm^4. Förster separation distance,R_0, corresponding to a rate of FRET, half the donor molecules decay by energy transfer and half decay by the usual radiative and non-radiative rates, is a function of the refractive index of the medium, η_D and the expression can be written in terms of following equation,

$$R_0 = \left(\frac{9000(\ln 10)k_p^2 Q_D}{128 N_A \pi^5 \eta_D^4} J(\lambda)\right)^{1/6} \tag{1.5}$$

The above expressions indicate that a quantum yield is necessary for determination of the Förster distance. The FRET efficiency, E_{ET}, is the fraction of photons absorbed by the donor which are transferred to the acceptor could be express as in equation,

$$E_{ET} = \frac{k_T(r)}{\tau_D^{-1} + k_T(r)} = \frac{R_0^6}{R_0^6 + r^6} \tag{1.6}$$

accounts for the fraction of excitons transferred from donor to acceptor non-radiatively. The efficiency can be experimentally measured by monitoring changes in the donor or/and acceptor fluorescence intensities, or changes in the fluorescent lifetimes of the fluorophores using the following expression,

$$E = 1 - \frac{F_{DA}}{F_D} = 1 - \frac{\tau_{DA}}{\tau_D} \tag{1.7}$$

where, the fluorescence intensity of the donor in the absence and presence of acceptor are F_D and F_{DA} and the lifetimes under these respective conditions are τ_{DA} and $\tau_D$respectively. FRET is a powerful photophysical technique and has been extensively used in the variety of investigations in the different field of sciences.

1.4.2. Gersten-Nitzan (GN) Model

Coinage metal nanoparticles have large extinction coefficient and could act as quencher as well as field enhancer for a fluorescing molecule. Based on this theory, Gersten-Nitzan in 1981, explained the phenomenon of surface enhanced fluorescence, when a fluoroprobe molecule was placed in the vicinity of a metal nanoparticle or on rough metal surfaces or on metal island films[31]. The observed phenomenon of surface enhance fluorescence is assumed to be a result of the modified local electromagnetic field around the fluorophore due to the shape, appearance and surface plasmon resonance effects of the metal. The fluorophore is assumed to behave as point dipole based on classical theory and placed at a distance, R from the particle center of radius r, such that, r << λ.

Assuming that the particle is very small compared to the wavelength of light (λ), under the consideration of the electrostatic theory, the metal-fluorophore assembly is considered as a complete system with a dipole moment which has contributions from both the metal and the fluorophore. The generation of the induced dipole due to the electric field of the metal causes, further, enhancement effect that is prominent at distances nearer to the surface. The field of the metal particles affects both the radiative decay, k_r and causes to act as an acceptor of energy to the metal particles. Ignoring the change in the radiative rate,k_r, energy transfer, k_{ET} would be the dominant process. Then, the Gersten-Nitzan energy transfer could be considered from 50% energy transfer rate and could be written as,[31,34]

$$R_0^{GN} = \left[2.25\ \frac{c^3}{\omega_{dye}^3} \cdot \Phi_{dye} \cdot\ r^3 \cdot\ \frac{(\epsilon_1+2)^2+\epsilon_2^2}{|\epsilon_2|^2}\right]^{1/6} \qquad (1.8)$$

where, ω_{dye} and Φ_{dye} is the frequency and quantum yield of the donor dye, r the radius of the metal nanoparticle, ϵ_1 and ϵ_2 are the real and imaginary part of the dielectric constant of the metal and c is the speed of light. The enhancement effect can be explained by

considering the native quantum yield (Φ_{dye}) of a fluorophore and can be written in terms of the radiative, k_r and non-radiative, k_{nr}decay rates of the fluorophore molecule.

$$\Phi_{dye} = \frac{k_r}{k_r + k_{nr}} \tag{1.9}$$

and the life time τ_{dye} is express as,

$$\tau_{dye} = \frac{1}{k_r + k_{nr}} \tag{1.10}$$

therefore, $$\Phi_{dye} = k_r \cdot \tau_{dye}. \tag{1.11}$$

The presence of fluorophore in the vicinity of metal nanoparticles provides another nonradiative pathway for loss of energy with modified quantum yield Φ'_{dye} and lifetimes,τ'_{dye} are,

$$\Phi'_{dye} = \frac{k_r}{k_r + k_{nr} + k_{ET}} \tag{1.12}$$

$$\tau'_{dye} = \frac{1}{k_r + k_{nr} + k_{ET}} \tag{1.13}$$

$$\Phi'_{dye} = k_r \cdot \tau'_{dye}. \tag{1.14}$$

The quantum yield and lifetime decreases when there is no change in the radiative rate,k_r, and an enhancement is observed when the field of the particle affects the radiative rate. The non-radiative paths are a collection of the vibrational and rotational pathways and are independent of the presence of any acceptor. Based on the assumptions of Gersten-Nitzan theory, the enhancement can be calculated in terms of an enhancement factor, η such that,

$$\eta = A(\lambda)\frac{\Phi'_{dye}}{\Phi_{dye}} - 1 \tag{1.15}$$

where, $A(\lambda)$ is the field enhancement factor related to the dielectric of the metal, *r* the radii of the metal nanoparticles and *R* the distance from the center of the particle to the fluorophore. Specifically, A(λ) could be expressed in the form,

$$A(\lambda) = 1 + 2\left|\frac{\epsilon(\lambda)-1}{\epsilon(\lambda)-2}\right|^2\left(\frac{r}{R}\right)^6 \tag{1.16}$$

The enhancement, thus, follows a directly dependent function on the size of the particle and inversely dependent function of the distance from the center of the particle to the fluorophore.

1.4.3. CPS-Kuhn Model

Metal thin films and their effects on a proximal fluorophore have been studied and postulated as the prominent theories by Kuhn in the year of 1970.[32] The theory explains the quenching of an emitting fluorophore when placed to the vicinity of a thin metal film and is applicable when the thickness (d) is less than the distance of the flurophore from surface (R) of the film. The fluorophore is treated as simple harmonic oscillator and the metal film is considered as a perfect mirror.

The classical theory of an oscillating charge distribution near a dielectric interface is applied to the variation of properties of fluorescing molecules near a metal surface. The non-radiative energy transfer to a nearby metal surface can be an effective decay channel for an excited molecule. The considerations of dipole-dipole transfer predict the inverse cubic dependence on distance, and the decay rate constant determined experimentally and is generally written as,

$$F = \beta d^{-3} \tag{1.17}$$

A theoretical assessment of β being proceeds along the lines of Förster energy transfer theory. This procedure is valid for weak absorbers but fails in the case of metals. However, the energy transfer rate constant for a perpendicular dipole is valid for all distances for both weak and metallic acceptors. For thick film, the energy-transfer rate constant varies as $d^{-3}$and for thin films, the energy transfer rate constant should vary as d^{-4}**,** or β will be proportional to d^{-1}.

The lifetime of an excited fluorophore near an interface between two media can be altered significantly due to reflection and absorption at the surface when the probe molecules were placed at a known fixed distance from the metal surface and were excited to record the fluorescence. It was observed that for large distances from the metal surface, the fluorescence lifetime oscillated as a function of distance, while for smaller distances the lifetime changes monotonically towards zero.[35] The oscillations are explained qualitatively as a mirror for the electric field of the fluorophore due to the metal surfaces. The lifetime decreases when the distance becomes small due to nonradiative transfer of energy from the excited fluorophore to the metal. The emitting molecule acts as an oscillating dipole (antenna) near a partially absorbing and partially reflecting metal

surface. It is seen that the surface-plasmon modes of the metal dielectric interface coupled to the near field of the emitting molecule.

The emitting field from the donor fluorophore induces oscillations in the acceptor which further generates induced field in the acceptor that travels back to the donor and reduces the acceptor oscillator. Thus, from Kuhn's theory, it can be assumed that the quenching is a retardation effect on the fluorophore due to the acceptor. The quenching of a quadruple emitter by thin film acceptor of metal has been explains by this theory. The Kuhn's theory of energy transfer was further modified by Chance, Prock and Silbey, the formula that gives the correct d^{-4} dependence and the expression can be written as,

$$k_{ET} = \frac{d_0^4}{d^4} \tag{1.18}$$

where, the critical transfer distance, d_0 can be given as,

$$d_0 = \frac{\alpha\lambda}{n}(Aq)^{1/4}\left[\frac{n_r}{2n_1}\left(1 + \frac{\varepsilon_1^2}{|\varepsilon_2|^2}\right)\right]^{1/4} \tag{1.19}$$

where, A is the absorbance of the metal film,

$$A = \frac{4\pi kd}{\lambda} \tag{1.20}$$

and the geometric factor, $\alpha = (1/4\pi)(9)^{1/4}$ for the dipole orientation is perpendicular and $\alpha = (1/4\pi)\left(\frac{9}{2}\right)^{1/4}$ for dipole orientation is parallel to the metal surface, λ emission wavelength of the donor dipole, ε_1, ε_2 the real and imaginary components of dielectric constant, $n_r$and n_m are refractive index of the metal and medium, d the thickness of the metal film respectively.[32,34-36] The dielectric constants are not size-dependent in CPS-Kuhn's assumption[35] which were further modified by incorporating the size dependence of the dielectric constants and can be accounted for by substituting a size dependent term for the dielectric constants[15]

1.4.4. Nanometal Surface Energy Transfer (NSET)

The nanometal surface energy transfer model is an extended theory proposed by Persson and Lang in 1982 where quenching behavior of a metal surface on an oscillating dipole was studied.[33] The metal is treated within the jellium approximation, i.e., the metal conduction electrons are assumed to move in a semi-infinite positive background obtained by smearing out the positive metal-ion core. The vibrational frequency of the

dipole (ω_{dye}) is smaller than the plasma frequency (ω_p) of the metal. In this region, since $\omega_{dye} << \omega_{p,}$ the conduction electrons of the metal can respond adiabatically to the slowly varying external field and thus, adjust to the instantaneous static configuration. The theory explains the damping effects of the metal surface and the rate of damping, $k_{ET}(= 1/\tau)$, i. e., the rate of vibrationally excited state ($n = 1$) decays to its ground state ($n = 0$), whereas, an electron is scattered from a level $\vec{k}$ below the Fermi surface ($k < k_F$) to a level $\vec{k}'$ above the Fermi surface $\vec{k}' > k_F$ as obtained from Golden-rule formula. For large distance range, such that, $d >> \omega_F/\omega_{dye}k_F$, the main contribution to the damping rate arises from the surface, where, ω_F is the Fermi frequency and k_F is the Fermi wave-vector for the metal. This theory also predicts that surface contribution due to rate of damping of the metal is different than with the volume contribution due to scattering of electrons against phonons, impurities. Thus, the effects of surface and core electrons could be considered individually and makes extremely applicable to the metal nanoparticle quenching, i. e., the rate of surface quenching is a function of the electron gas density parameter (r_s) while the volume damping is a function of the bulk dielectric function arising from the scattering of the electrons against the phonons, impurities etc. The generalized damping can be written as,

$$k_{ET} = \frac{1}{\tau} = \frac{\mu^2}{4d^3\hbar}F \tag{1.21}$$

where, μ is the dipole moment of the emitter, d the distance of the emitter from the metal surface and F is damping/quenching term of the surface and volume and thus, could be expressed as,

$$F_{surface} = 1.2\ \frac{\omega_{dye}}{\omega_F}\frac{1}{k_F d} \tag{1.22}$$

and

$$F_{volume} = 3\ \frac{\omega_{dye}}{\omega_F}\frac{1}{k_F l} \tag{1.23}$$

Therefore, the volume quenching is a function of $1/d^3$ and the mean free path, $l(= v_F\tau')$ for the metal while the surface quenching is a $1/d^4$ dependent phenomenon. The surface and the volume are indistinguishable for very small particles and hence, surface quenching is observed whereas larger particles have a well formed surface and a distinguishable volume. As a consequence, surface quenching is expected at shorter

distances while volume quenching plays a dominant role at longer distances. For metals having extremely long mean free paths, surface quenching is the leading contributor at distances up to 300 Å. Based on these approximations and results, the critical distance d_0 value is calculated and the expression could be written as,[37]

$$d_0 = \left(0.225\ \frac{\Phi_{dye}}{\omega_{dye}^2}\frac{c^3}{\omega_F k_F}\right)^{1/4} \tag{1.24}$$

where, ω_{dye} and Φ_{dye} represent the angular frequency of donor emission and the quantum yield of the donor, ω_F is the vibrational frequency of dipole for bulk gold (8.4×10^{15} s^{-1}), k_F is the Fermi wave vector for bulk gold (1.2×10^8 cm^{-1} and $c = 3.0 \times 10^8$ ms^{-1} is the speed of light.[37]

1.5. Experimental Observation

The modification of the surface by the adsorption of varieties of organic fluorophores onto the surface alters the physical properties or the surface functionalities changes the emission properties of the fluorophores as well as the radiative rate under the influence of an enhanced electromagnetic field arising from the particles. Organic fluoroprobes have often been attached near the nanosurface to measure the surface plasmon fields. The intensity of the surface plasmon fields have a maximum value/peak point at the interface and exponentially decayed in the directions perpendicular to the interface.[38] The rate of fluorescence of molecular probes in the close proximity of a metal is a function of the distance between the fluoroprobe and the metal surface. The fluorescence of molecules in direct contact with the metal is completely quenched. In the presence of aggregated metal clusters, the applied electromagnetic field results the enhancement of radiative decay rates and quantum yields significantly. Therefore, to design an experiment, it is necessary that the adsorbed molecule minimizes the surface damage by the laser/electromagnetic radiation and there should not be any photochemical decomposition of the fluoroprobe near the metal surface.

1.5.1. Fluorescence Quenching

There have been several reports on fluorescence quenching of molecular probes near the surface of metallic nanoparticles in the literature.[39-41] Dulkeith et al.[19] measured the radiative and nonradiative decay rates of lissamine dye molecules chemically attached to

differently sized gold nanoparticles by means of time-resolved fluorescence experiments. Fan and and group[42] have reported the conjugated polymer–gold nanoparticle pairs which exhibit an extraordinary quenching efficiency. Kamat and colleagues have described the fluorescence of the chromophores of pyrene derivatives on the surface of gold nanoparticles.[25] Chen and Chang[43] observed highly fluorescent products forming from the assembly of nile red onto citrate-stabilized gold nanoparticles. Makarova et al.[44] have reported the co-adsorption of fluorescein isothiocyanate dye molecules onto the surface of gold nanoparticles modified with 3-aminopropyltrimethoxysilane.

The quenching phenomenon could be explained by the electromagnetic coupling between the metal and the fluoroprobe molecules using Weitz theory.[45] According to this theory, the scattering intensity ratio for fluorescence of adsorbed molecules to that of the free ones is given by,

$$R_{fluo} = |A(\omega_L)|^2 |E_L|^2 \frac{\Gamma_0}{\Gamma_0 + \Gamma_0^s} \tag{1.25}$$

where, E_L is local electric field at the molecule due to the incident laser radiation. The amplification factor, $A\,(\omega_L)$ is increases local field intensity through the excitation of electronic plasmon resonances and is controlled by the morphology and dielectric properties of the particles. The parameter, Γ_0 denotes the radiative and non-radiative transition rate from the excited state to the ground state for free molecules while Γ_0^s represents an average value of the surface-induced decay rate for molecules on the gold nanoparticles. The radius-dependent fluorescence decay rate $R_{fluo}(r)$ can be expressed as,[19]

$$R_{fluo}(r) = R_{rad}(r) + R_{nonrad}(r) \tag{1.26}$$

and the fluorescence quantum efficiency $E(r)$ as,

$$E(r) = R_{rad}(r)/R_{fluo}(r) \tag{1.27}$$

At very small distances (1–2 nm), the very high fluorescence quenching efficiency is due to two factors: firstly, gold nanoparticles increase the nonradiative rate, R_{nonrad} of the molecules due to energy transfer, and secondly, the radiative rate, R_{rad} of the molecules is decreased because the molecular dipole and the dipole induced on the gold nanoparticles radiate out of phase if the molecules are oriented tangentially to the gold nanoparticle's surface. When the distance is very long, the distance dependent quantum

efficiency is almost completely governed by the radiative rate. However, the adsorption of the probe molecules onto the nanoparticle surface is dependent on the chemical composition, structure and size of the metal particles, along with the nature of the solution.[46]

1.5.2. Fluorescence Enhancement

There have been several reports on the fluorescence enhancement of fluoroprobe molecules nearby metal surface in the literature.[47-52] The fluorescence enhancement of dye molecules near to the metallic surfaces was reported first by Glass et al.[53] in 1980 and later confirmed by other groups.[54, 55,] George Thomas and Kamat[56] have reported the surface binding of amine groups of 1-aminomethylpyrene chromophores on gold nanoparticles in which the intramolecular charge-transfer interactions between the amine group and the pyrene chromophore was suppressed and thereby, enhancing the fluorescence yield. Kinkhabwala have reported[57] the 1340-fold intensification of the fluorescence enhancement of fluorophore molecules placed in the gap of a gold bowtie antenna**.**

Metallic nanoparticles may lead to the fluorescence enhancement that placed in the vicinity of a metal surface.[58] The emission of nearby fluorophores could be drastically changed by enhancing the optical intensity, by modifying the radiative decay rate and/or by increasing the coupling efficiency of the fluorescence emission. These could be controlled by separation between molecule to nanoparticles, size of nanoparticles, and the morphology. Metal nanostructures have the ability to concentrate incident light into a very small volumes that allows the enhancement of the local density of states (LDOS) and consequently, enhance the decay rate of an emitter. When light is concentrated into a sub-diffraction volumes, the electromagnetic radiation field intensified leading to the formation of 'hot spots'[59,60] where the intensity of the incident light enhanced up to 1000 times as compared to the incident volume. Thus, placing a molecule in a 'hot spot' improves the efficiency which further enhances the optical excitation process. If a fluorescing dye molecule is placed in the hot spot, the detection signal of the fluorescence enhancement, f_F, can be written in form of following expression as,

$$f_F = \frac{\eta}{\eta_0} \frac{|\mu_{if}.E_{loc}|^2}{|\mu_{if}.E_0|^2} \tag{1.28}$$

where E_0 and E_{loc} are the incident and local electric fields at the molecule position, η and η_0 are the quantum efficiency of the molecules[61,62] close to and far from the nanostructures. The quantum efficiency is defined as the ratio between the radiative decay rate, γ_r, to the total decay rate of the molecule, $\gamma(=\gamma_r+\gamma_{nr})$, and could be written as,

$$\eta = \frac{\gamma_r}{\gamma} = \frac{\gamma_r}{\gamma_r+\gamma_{nr}} \tag{1.29}$$

The nonradiative decay rate, γ_{nr}, specifies the absorption in the metal nanostructures and other intrinsic losses. Due to the formation of hot spot, the local field, E_{1oc}, is very large compared with the applied field that leads the strong enhancement of fluorescence intensity and the value of f_F will be maximum only when both the quantum efficiency (η/η_0) and the local electromagnetic field are amplified. The quantum efficiency and the near-field enhancement are evaluated at two different frequencies that contribute to the fluorescence amplification. The incident frequency of the electric field factor, $(|\mu_{if}.E_{loc}|^2/|\mu_{if}.E_0|^2)$, is calculated that excites localized surface plasmon resonance of the absorption wavelength of the emitter and the quantum efficiency, (η/η_0), enhancement is calculated at the emission frequency.

1.5.3. Simultaneous Quenching and Enhancement

The capping agents play the key role in controlling the distance between the metal particles and the probe molecules on the nanometer scale. Longer the chain length of the surfactant molecules electrostatically bound to the particles reduces the donation of electrons from a fluoroprobe to the gold surface and at optimum distance quenching and enhancement of fluorescence can be observed. Zhao et al.[50] have observed simultaneous quenching and enhancement in a system of C_{60}/C_{70}-pyridine-gold hydrosol. The energy transfer between C_{60} molecules and gold nanoparticles leads to the quenching of fluorescence bands centered at 450 nm while the fluorescence bands at 700 nm of C_{70} are enhanced arising from the increased local field intensity through the excitation of surface plasmon resonance of gold nanoparticles. The emission of molecular fluorescence is influenced by modification of the radiative decay rate by the nearby metallic nanoparticles which simultaneously alter the quantum yield similar to the effect of nearby macroscopic metallic surface. Coupling of the fluorescent emission to the far field is

influenced by the scattering efficiency of the metallic nanoparticles that depends on the size of the particles as well. Therefore, under suitable conditions, the luminescence properties of the fluorophores are dominated over the quenching effect especially by the highly localized near field interactions, leading to fluorescence enhancement of the probe molecules on the surface of metallic nanostructures.

1.6. Photophysical Processes

When fluoroprobes molecules are placed in the vicinity of metal nanoparticles and allow to incident the electromagnetic radiation, several possible deactivation pathways

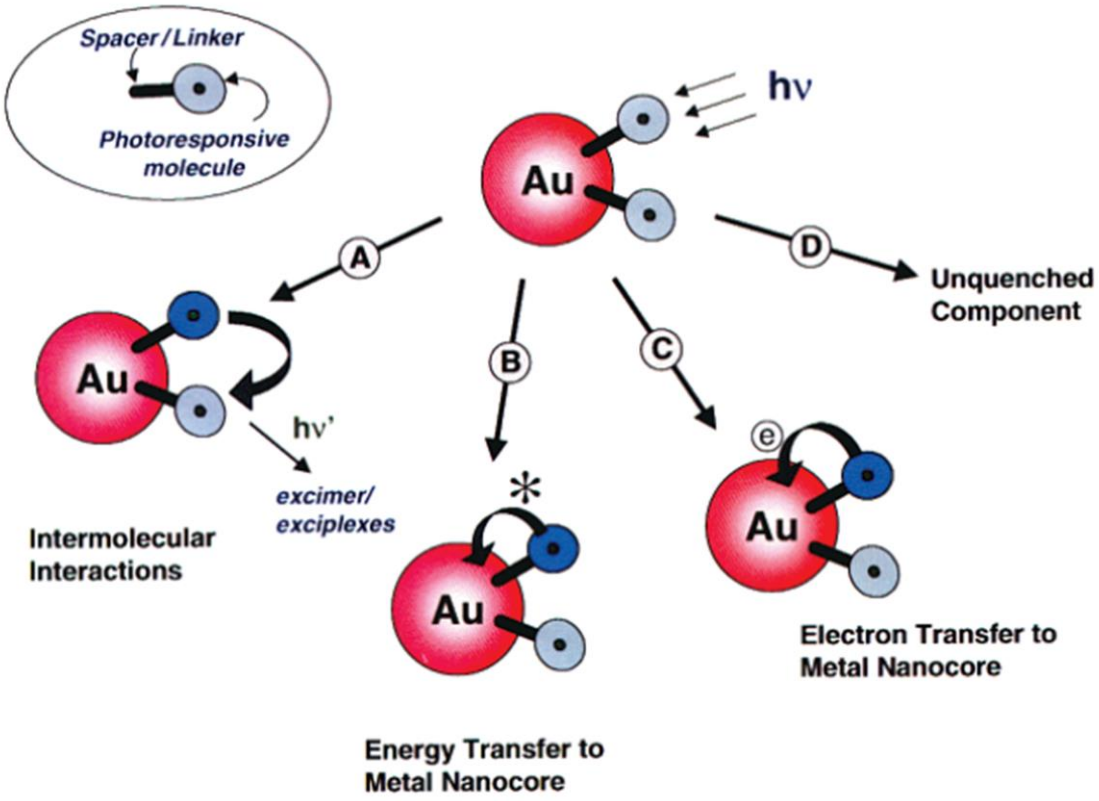

Figure 1.2. Excited-state deactivation processes in metal-fluorophore nanohybrids. (Reproduced from Ref. 25)

may be followed. The possible deactivation pathways[24] of the photoexcited fluoroprobe could be summarized as the intermolecular interactions, energy transfer, electron transfer and the emission from the fluoroprobes near the surface of the metal. Direct experimental measurements of these concepts are needed to validate theoretical predictions and to develop systems with improved fluorescence properties.

1.6.1. Intermolecular and Intramolecular Interaction

The excited state interaction could be manipulated by varying the coverage of the photoresponsive molecules around Au nanoparticles. The flexible linker between the nanoparticle and the fluorophore unit offers a topographical control of fluorophore interaction between themselves in the three-dimensional monolayers. This may also lead to the formation of the dimer in the excited state and excimer emission and absorption observed at higher fluorophore loading on the surfaces. It has also been seen that the self-assembled monolayers of stilbene derivatives undergo dimerization on planar gold, indicating, the ω-functionalized fluorophores are loosely packed onto the gold nanoparticles. From these studies, it can be concluded that the nature of the linker provides a topographical control of the different interactions on the three-dimensional surface of metal nanoparticles leading to the formation of various types of intramolecular complexes.[25]

1.6.2. Electron Transfer

Noble metals nanoparticles exhibit increasing photochemical activity due to their high surface-to-volume ratio and unusual electronic properties. Photoactive molecules bind to metal nanoparticles to form organic–inorganic hybrid nanoassemblies and exhibit greater photoactivity. The metals, in the nanoscale, are more electronegative and possess very high residual force than the bulk material. As a result, the metallic particles could participate in the electron transfer process and the effect is predominant for particle sizes <5 nm.[63] For the particles, in the size range of <5 nm, the surface area sharply increases and they do not exhibit any surface plasmon band in the visible region.[14] The nature of charge transfer from fluorophore to gold surface directs the pathways through which the excited-state deactivates. The gold atoms on the surface possess unoccupied orbitals and therefore, have the residual force to accept electrons from fluoroprobes capable of donating lone pair electrons. Moreover, efficient electron transfer from the probe molecules to the metal surface may happen that causes the ‘‘superquenching’’ of the molecular fluorescence over the metal surface.[42] Moreover, due to strong surface-like character of the nanoscale metallic particles, the fluoroprobe molecules could be employed to measure the distance of the probe molecules above the interface.[64,65]

1.6.3. Energy Transfer

Energy transfer is a useful technique in biophysics, biochemistry and in molecular biology to determine the nature of binding, the distances between the nanoparticle and the fluorescent probe and the dynamic interaction with high accuracy in single molecule level.[66] Resonance energy transfer efficiency is high till the quencher–fluorophore pair separation approaches the Förster radius, R_0 (typically~10 nm). The energy transfer could be obtained directly from Fermi-Golden rule that relates the energy transfer rate (k_{ET}) to a product of the interaction elements of the donor (F_D) and acceptor (F_A), $k_{EnT} \approx F_D F_A$. These interaction elements can be simplified such that their separation distance (d) dependencies are sole functions of their geometric arrangement. For single dipoles, $F \approx 1/d^3$, for a 2D dipole array, $F \approx 1/d$, and for a 3D dipole array, $F = constant$ such that the power of the distance factor decreases as the dimensions increases.[33] Förster resonance energy transfer consists of two single dipoles such that $k_{FRET} \approx F_D F_A \approx (1/d^3)(1/d^3) \approx 1/d^6$, where, d is the surface-to-surface distance between the metallic nanoparticle and the probe molecule. Indeed, FRET is generally expressed as, $k_{FRET} \approx \left(1/\tau_D\right)(R_0/r)^6$, where τ_D is the lifetime of the donor. The details of FRET have been explained in section 1.4.1. The NSET is based on the Pearson model that has been experimentally demonstrated by Strouse[67] in which a long-range molecular ruler consisting of an organic dye donating energy to a nanosurface and the rate of energy transfer rate from the dipole to surface of the metal can be expressed as, $k_{NSET} \approx F_D F_A \approx (1/d^3)(1/d) \approx 1/d^4$ and the exact form of dipole-surface energy transfer is $k_{NSET} \approx \left(1/\tau_D\right)(d_0/d)^4$, where, d_0, the characteristic distance length is a function of the donor quantum efficiency as explained in section 1.4.4. The interaction of fluorophores with metal surfaces is changed with distance regime. At very close distances(< 10Å), radiative rate enhancement is observed; at intermediate distances ($20-300$ Å), energy transfer is the dominant process; and at very large distances(> 500 Å), fluorescence oscillations due to dipole-mirror effects take precedence. The general expression of the efficiency of energy transfer can be written as,

$$E_{ET} = \frac{1}{1+\left(\frac{r}{r_0}\right)^n} \tag{1.30}$$

where, FRET (dipole-dipole), $n = 6$ and $r_0 = R_0$, and NSET (dipole-surface), $n = 4$ and $r_0 = d_0$. The nature of the energy transfer mechanism can be obtained from the slope of a plot of energy transfer efficiency *vs.* separation distance of the donor and acceptor. The theoretical details of energy transfer have been explained in section 1.4. Metals, in the nanoscale dimension, have a continuum of electronic states (quantum size effect) and act as excited state quenchers. The closest distance of the probe molecules to the nanoparticle core will change with size of the particles. Therefore, the quenching process is dependent on the nanoparticles dimension and lies in the core-size related differences in the density of the electronic states of the gold nanoparticles.[40] In efficient quenching processes, the energy transfer from molecules to the gold nanoparticles of the excited state and transfer to the ground state non-radiatively and increases the surface energy of gold that released as Joule heat.[42] The chemisorption of the probe molecules to the gold surface leads to the mixing of the molecular orbitals of the probe molecules with the metallic band states. Therefore, the energy transfer in quenching is a sensitive to the density of electronic state changes of the metal particles.

1.7. Application of Metal Probe Hybrid Assembly

While shrinking the dimensions of particles to lesser than the wavelength of the exciting light, energy can be confined and enhanced in small volume through the photon of local excitation of surface plasmon resonances.[1] Based on the optical and electronic properties using surface plasmon mode, nanoscience and nanotechnology have the impact in biophotonics and in material science through radiative decay engineering of organic molecules nearby the conducting metal surfaces.[17] The enhanced detectability and photostability of fluorophores has improved DNA detection and molecular protein labeling and their self-quenching of fluorescence of the molecular probe over labeled proteins, enhanced wavelength-ratiometric sensing, and the metallic surfaces applied to amplified with ultrafast and high sensitivity to assay detection and diagnostic technology.[68] The enhanced fluorescence of the fluoroprobes around nanosurface improves the sensitivity of fluorophore-mediated biosensors and thus, acting as effective signal mediator for fluorophore-mediated bioimaging as well as biosensing.[14] Photothermal therapy of cancer using NIR absorbing gold nanorods with tunable aspect ratio provides localized and targeted approaches with enhance efficacy reducing side

effects and improves the quality of life of the patients.[2,69] Nanosurface energy transfer based miniaturized fluoroprobes for rapid and ultrasmall detection of mercury from different samples have been observed with excellent sensitivity and selectivity for the development of a practical nanosensor for screening from a wide range of biological, toxicological, and environmental samples.[70] The biosensing process based on nanometal surface energy transfer signals between quantum dots and gold nanoparticles bound to specific sialic acid binding protein and its moieties can be utilized to detect and quantify with high selectivity up to micromolar level of the linkers.[71] The science of immunology provides the rational manipulation/modulation of the immune system with nanoparticles-based strategy to enable effective and safer immune engineering at the cellular and molecular level over the traditional drug development approaches. The increase in localization of nanoparticles probing antigen with intrinsic immunomodulatory function, exert effect in target tissue or immune cells by changing the functions like crosslinking, intercellular processing, cytosolic delivery, physical co-localizing synergistic signals within intracellular or in surface and acting as adjuvants or immune potentiators.[3]

1.8. References

(1) Schuller, J. A.; Barnard, E. S.; Cai, W.; Jun, Y. C.; White, J. S.; Brongersma, M. L. *Nat. Mater.* **2010**, *9*, 193−204.

(2) Kennedy, L. C.; Bickford, L. R.; Lewinski, N. A.; Coughlin, A. J.; Hu, Y.; Day, E. S.; West, J. L.; Drezek, R. A. *Small* **2010**, *7*, 169−183.

(3) Irvine, D. J.; Hanson, M. C.; Kavya Rakhra; Tokatlian, T. *Chem. Rev.* **2015,** *115*, 11109–11146.

(4) Giannini, V.; Fernández-Domínguez, A. I.; Heck, S. C.; Maier, S. A. *Chem. Rev.* **2011**, *111*, 3888–3912.

(5) Chinen, A. B.; Guan, C. M.; Ferrer, J. R.; Barnaby, S. N.; Merkel, T. J.; Mirkin, C. A. *Chem. Rev.* **2015,** *115*, 10530–10574.

(6) Mayer, K. M.; Hafner, J. H. *Chem. Rev.* **2011**, *111*, 3828–3857.

(7) Morton, S. M.; Silverstein, D. W.; Jensen, L. *Chem. Rev.* **2011**, *111*, 3962–3994.

(8) Rycenga, M.; Cobley, C. M.; Zeng, J.; Li, W.; Moran, C. H.; Zhang, Q.; Qin, D.; Xia, Y. *Chem. Rev.* **2011**, *111*, 3669–3712.

(9) Shalaev, V. M. *Science* **2008**, *322*, 384-386.

(10) Brongersma, M. L.; Shalaev, V. M. *Science* **2010**, *328*, 440-441.

(11) Gramotnev, D. K.; Bozhevolnyi, S. I. *Nat. Photonics* **2010**, *4*, 83-91.

(12) Lal, S.; Link, S.; Halas, N. J. *Nat. Photonics* **2007**, *1*, 641-648.

(13) Barnes, W. L.; Dereux, A.; Ebbesen, T. W. *Nature* **2003**, 424, 824-830.

(14) Ghosh, S. K.; Pal, T. *Chem. Rev.* **2007**, *107*, 4797–4862.

(15) Kreibig, U.; Vollmer, M. Optical Properties of Metal Clusters. Springer, Verlag, Berlin, 1995.

(16) Mie, G. *Ann. Phys.* **1908**, *25*, 377- 445.

(17) Geddes, C. D.; Aslan, K.; Gryczynski,I.; Malicka, J.; Lakowicz, J. R. Radiative Decay Engineering, in Topics in *Fluorescence Spectroscopy*, Kluwer Academic/Plenum Publishers, New York, 2005.

(18) Chanaewa, A.; Schmitt, J.; Meyns, M.; Volkmann, M,; Klinke, C.; von Hauff, E. *J. Phys. Chem. C* **2015**, *119*, 21704–21710.

(19) Dulkeith, E.; Morteani, A. C.; Niedereichholz, T.; Klar, T. A.; Feldmann, J.; Levi, S. A.; van Veggel, F. C. J. M.; Reinhoudt, D. N.; Moller, M.; Gittins, D. I. *Phys. Rev. Lett.* **2002**, *89*, 203002 1–4.

(20) Dubertret, B.; Calame, M.; Libchaber, A. J. *Nat. Biotechnol*. **2001**, *19*, 365–370.

(21) Zenneck, J. *Ann. Phys*. **1907**, *328*, 846–866.;

(22) Sommerfeld, A. *Ann. Phys.* **1909**, *28*, 665–736.

(23) Morawitz, H.; Philpott, M. R. *Phys. Rev. B* **1974**, *10*, 4863–4868.

(24) Kamat, P. V. *J. Phys. Chem. B* **2002**, *106*, 7729–7744.

(25) George Thomas, K.; Kamat, P. V. *Acc. Chem. Res.* **2003,** 36, 888−898.

(26) Selvin, P. R. *Nat. Struct. Biol.* **2000**, *7*, 730-734.

(27) Clapp, A. R.; Medintz, I. L.; Mattoussi, H. *Chem. Phys. Chem.* **2006**, *7*, 47−57.

(28) Lakowicz, J. R. Principles of *Fluorescence Spectroscopy*, Springer Science, 2006.

(29) Sapsford, K. E.; Berti, L.; Medintz, I. L. *Angew. Chem. Int. Ed.* **2006**, *45*, 4562-4588.

(30) Förster, T. *Ann. Phys*. **1948**, *437*, 55 −75.

(31) Gersten, J.; Nitzan, A. *J. Chem. Phys.***1981**, *75*, 1139−1152.

(32) Kuhn, H. *J. Chem. Phys.***1970**, *53*, 101−108.

(33) Persson, B. N. J.; Lang, N. D. *Phys. Rev. B* **1982**, *26*, 5409−5415.

(34) Singh, M. P.; Strouse, G. F. *J. Am. Chem. Soc.* **2010**, *132*, 9383−9391.

(35) Chance, R. R.; Prock, A.; Silbey, R. *Adv. Chem. Phys.* **1978**, *37*, 1−65.

(36) Inacker, O.; Kuhn, H. *Chem. Phys. Lett.* **1974**, *27*, 317−321.

(37) Jennings, T. L.; Singh, M. P.; Strouse, G. F. *J. Am. Chem. Soc.* **2006**, *128*, 5462−5467.

(38) Ghosh, S. K.; Pal, T. *Phys. Chem. Chem. Phys.* **2009**, *11*, 3831–3844.

(39) Förster, T.; Kasper, K. *J. Phys. Chem.*, **1954**, *1*, 275–277.

(40) Aguila, A.; Murray, R. W. *Langmuir* **2000**, *16*, 5949–5954.

(41) Templeton, A. C.; Cliffel, D. E.; Murray, R. W. *J. Am. Chem. Soc.* **1999**, *121*, 7081–7089.

(42) Fan, C.; Wang, S.; Hong, J. W.; Bazan, G. C.; Plaxco, K. W.; Heeger, A. J. *Proc. Natl. Acad. Sci.* U. S. A. **2003**, *100*, 6297–6301.

(43) Chen, S. J.; Chang, H. T. *Anal. Chem.* **2004**, *76*, 3727–3734.

(44) Makarova, O. V.; Ostafin, A. E.; Miyoshi, H.; Jr, Norris, J. R.; Meisel, D. *J. Phys. Chem. B* **1999**, *103*, 9080–9084.

(45) Weitz, D. A. ; Garoff, S.; Gersten, J. I.; Nitzan, A. *J. Chem. Phys.* **1983**, *78*, 5324–5338.

(46) Zhang, H.; Penn, R. L.; Hamers, R. J.; Banfield, J. F. *J. Phys. Chem. B* **1999**, *103*, 4656–4662.

(47) Wang, T.; Zhang, D.; Xu, W.; Yang, J.; Han, R.; Zhu, D. *Langmuir* **2002**, *18*, 1840–1848.

(48) Enderlein, J. *Appl. Phys. Lett.* **2002**, *80*, 315–317.

(49) Enderlein, J. *Phys. Chem. Chem. Phys.* **2002**, *4*, 2780–2786.

(50) Sershen, S. R.; Westcott, S. L.; Halas, N. J.; West, J. L. *J. Biomed. Mater. Res.* **2000**, *51*, 293–298.

(51) Sershen, S. R.; Westcott, S. L.; West, J. L.; Halas, N. J. *Appl. Phys. B* **2001**, *73*, 379–381.

(52) Zhao, Y.; Jiang, Y.; Fang, Y. *Chem. Phys.* **2006**, *323*, 169–172.

(53) Glass, A. M.; Liao, P. F.; Bergman, J. G.; Olson, D. H. *Opt. Lett.* **1980**, *5*, 368–370.

(54) Geddes, C. D.; Gryczynski, I.; Malicka, J.; Lakowicz, J. R. *Noble Metal Nanostructure for Metal Enhanced Fluorescence,* In Review Chapter for Annual

Reviews in *Fluorescence*, Kluwer Academic/Plenum Publishers, New York, 2004, p. 365.

(55) Krenn, J. R. *Nat. Mater.* **2003**, *2*, 210–211.

(56) George Thomas, K.; Kamat, P. V. *J. Am. Chem. Soc.*, **2000**, *122*, 2655–2656.

(57) Kinkhabwala, A.; Yu, Z.; Fan, S.; Avlasevich, Y.; Müllen, K.; Moerner, W. E. *Nat. Photonics* **2009**, *3*, 654−657.

(58) Aravind, P. K.; Nitzan, A.; Metiu, H. *Surf. Sci.*, **1981**, *110*, 189–204.

(59) Novotny, L.; Hecht, B. *Principles of Nano-Optics*; Cambridge University Press: New York, 2006.

(60) Maier, S. A. *Plasmonics: Fundamentals and Applications*; Springer: New York, 2007.

(61) Kühn, S.; Håkanson, U.; Rogobete, L.; Sandoghdar, V. *Phys. Rev. Lett.* **2006**, *97*, 1−4.

(62) Anger, P.; Bharadwaj, P.; Novotny, L. *Phys. Rev. Lett.* **2006**, *96*, 113002 1−3.

(63) Shen, J.; Jia, J.; Bobrov, K.; Guillemot, L.; Esaulov, V. A. *J. Phys. Chem. C* **2015**, *119*, 15168 −15176.

(64) Aslan, K.; Gryczynski, I.; Malicka, J.;Matveeva, E.; Lakowicz, J. R.; Geddes, C. D. *Curr. Opin. Biotechnol.* **2005**, *16*, 55–62.

(65) Drexhage, K. H.; Kuhn, H.; Shäfer, F. P. *Ber. Bunsen-Ges.* **1968**, *72*, p. 329.

(66) Vogelsang, J.; Doose, S.; Sauer, M.; Tinnefeld, P. *Anal. Chem.* **2007**, *79*, 7367–7375.

(67) Yun, C. S.; Javier, A.; Jennings, T.; Fisher, M.; Hira, S.; Peterson, S.; Hopkins, B.; Reich, N. O.; Strouse, G. F. *J. Am. Chem. Soc.* **2005**, *127*, 3115-3119.

(68) Zhang, Y.; Aslan, K.; Previte, M. J. R.; Geddes, C. D. *Chem. Phys. Lett.* **2006**, *432*, 528–532.

(69) Huang, X.; Jain, P. K.; El-Sayed, I. H.; El-Sayed, M. A. *Lasers Med. Sci.* **2008**, *23*, 217–228.

(70) Darbha, G. K.; Ray, A.; Ray, P. C. *ACS Nano* **2007**, 1, 208–214.

(71) Kikkeri, R.; Padler-Karavani, V.; Diaz, S.; Verhagen, A.; Yu, H.; Cao, H.; Langereis, M. A.; De Groot, R. J.; Chen, X.; Varki, A. *Anal. Chem.* **2013**, *85*, 3864 −3870.